Hindawi
Journal of Food Biochemistry
Volume 2023, Article ID 8936119, 20 pages
https://doi.org/10.1155/2023/8936119

Research Article

Astragalus Polysaccharides Alleviate Lung Adenocarcinoma Bone Metastases by Inhibiting the CaSR/PTHrP Signaling Pathway

Xiaoting Ma, Cong Wang, and Jing Yu

Cancer Center, Beijing Friendship Hospital, Capital Medical University, No. 95 Yong An Road, Xi Cheng District, Beijing 100050, China

Correspondence should be addressed to Jing Yu; yujing026@ccmu.edu.cn

Received 6 October 2022; Revised 6 November 2022; Accepted 9 November 2022; Published 7 February 2023

Academic Editor: Jae Young Je

Bone metastasis is one of the common complications of lung cancer and can lead to bone-related adverse events, such as pathological fractures, spinal cord defects, and nerve compression syndrome. As an effective medicinal component of *Astragalus membranaceus*, *Astragalus* polysaccharide (APS) has antitumor activity and alleviates osteoporosis to a certain extent. In this study, we explored the possible role and mechanism underlying APS inhibition of lung adenocarcinoma bone metastases by constructing a mouse model of lung adenocarcinoma bone metastases. First, we constructed osteoclast (OC) and osteoblast (OB) culture systems *in vitro* to confirm that APS affected the differentiation and function of OCs and OBs. Then, using the mouse bone metastasis model, microCT, and bone histopathology, we confirmed that APS inhibited osteolytic metastasis and tumor cell proliferation in mice, and the effect was mainly realized by inhibiting the CaSR/PTHrP signal pathway. The results showed that APS had a protective effect on lung adenocarcinoma bone metastases.

1. Introduction

Lung cancer is characterized by a high incidence and mortality rate worldwide, and bone metastasis is the most common site of distant organ metastasis [1, 2]. Studies have shown that the incidence of bone metastasis in patients with advanced lung cancer is 30%40%, and pathological fractures, spinal paraplegia, and other severe bone metastasis-related events affect the prognosis of lung cancer patients and their quality of life [3, 4]. Lung cancer cells that migrate to the local bone tissue cannot directly cause osteolysis, but can have a variety of complex interactions with the local bone tissue microenvironment, then enhance the activity of osteoclasts (OCs), promote bone resorption, reduce the bone formation of osteoblasts (OBs), lead to an imbalance of homeostasis in the local bone microenvironment, and finally lead to the occurrence and development of bone metastases.

Studies have shown that the calcium ion (Ca^{2+}) concentration in peripheral blood plasma is between 2.2 and 2.6 mM, the Ca^{2+} concentration in bone is approximately 10 mM, and the Ca^{2+} concentration in extracellular bone tissue could reach 20 mM. This finding reflected the increase in Ca^{2+} concentration from the bone to the internal bone tissue [5, 6]. The G protein-coupled calcium-sensing receptor (CaSR) is an important calcium-binding receptor in bone tissue [7]. According to the "seed-soil" theory related to tumor metastasis, tumor cells with preferential bone metastasis often have some unique biological characteristics, while tumor cells without bone metastasis do not exhibit this characteristic. Studies have confirmed that tumor cells with high expression of CaSR were more prone to bone metastasis compared to tumor cells with low expression of CaSR [8, 9]. A bone microenvironment rich in Ca^{2+} can be used as a chemokine to recruit tumor cells with "unique biological characteristics"; high expression of CaSR reaches local bone tissue via epithelial-mesenchymal transition (EMT). Tumor cells directly or indirectly act on OCs in the bone microenvironment, break the balance of bone metabolism, promote the differentiation and maturation of OCs, initiate bone absorption, create space for tumor cell colonization and proliferation, and form new bone metastases. CaSR promotes tumor cells to secrete a parathyroid hormone-

related protein (PTHrP), which is closely related to tumor cell survival and invasion [10, 11]. Our previous study showed that CaSR induced the expression of receptor activator of nuclear factor-κB ligand (RANKL) on the surface of OBs and inhibited the expression of osteoprotegerin (OPG) in A549 cells with high metastatic potential, thus disrupting the balance of bone metabolism. In addition, CaSR promoted the differentiation and maturation of OCs. The mechanism may be related to the fact that CaSR activation promotes the expression of nuclear factor kappa-light-chain enhancer of activated B cells (NF-κB) and enhances the release of PTHrP, which ultimately promotes lung adenocarcinoma bone metastasis [12].

Astragalus membranaceus is a precious perennial herb that is widely distributed in temperate and arid regions of Asia, Europe, and North America. In traditional Chinese medicine, *Astragalus membranaceus* is also called "invigorating qi." Astragalus root is one of the most adaptable medicinal materials and can prevent harmful pathogens or disease factors from entering the body and support the body to detoxify. Moreover, *Astragalus membranaceus* is considered to be safe and nontoxic, and dosage of the LD50 is approximately 40 g/kg. The patent combination of *Astragalus membranaceus* and four kinds of herbs, including ginger, turmeric, red sage, and rhubarb, has been proven to be nontoxic in female rats of reproductive age with a dose of 430 mg/kg. *Astragalus* polysaccharide (APS), an important active ingredient of *Astragalus membranaceus*, directly or indirectly kills tumors or exhibits multiple antitumor activities in coordination with chemotherapy and has been of interest in cancer treatment due to its relatively low toxicity [13, 14]. A number of *in vivo* and *in vitro* studies have demonstrated that APS alleviated osteoporosis to some extent, which may be related to an ability to manipulate calcium homeostasis and improve the balance between OCs and OBs [15]. Therefore, we speculated that APS may also have an inhibitory effect on the occurrence and development of malignant tumor bone metastasis. *In vivo* studies have shown that APS inhibited NF-κB activity, while NF-κB had an important role in the occurrence, growth, development, and metastasis of cancer [16–18]. In addition, some studies have confirmed that APS inhibited metastasis of nonsmall cell lung cancer cells, which is clinically feasible [19, 20]. In this study, we constructed an OC and OB culture system *in vitro* and a murine model of lung adenocarcinoma bone metastasis to explore the effect and mechanism of underlying APS on inhibiting lung adenocarcinoma bone metastasis and to provide a theoretical basis for the comprehensive treatment model of lung adenocarcinoma bone metastasis.

2. Materials and Methods

2.1. Reagents and Antibodies. The purity of APS is >95%. APS was purchased from Shanghai Yuanye Biological Technology Company (Shanghai, China). *Astragalus* polysaccharide is a powder, water-soluble, and an active component of the polysaccharide extract of *Astragalus*. RANKL and macrophage colony-stimulating factor (M-CSF) were purchased from the R&D system. F-12K medium, the alpha modification of Eagle's medium (α-MEM), Dulbecco's modified Eagle's medium (DMEM), premium fetal bovine serum (FBS), and phosphate-buffered saline (PBS) were purchased from Hyclone (Logan, UT, USA). RIPA lysis buffer was purchased from Thermo Scientific (Wilmington, DE, USA). Neutral formaldehyde solution, alizarin red dye solution, and crystal violet dye solution were purchased from Sigma (St. Louis, MO, USA). Annexin V and propidium iodide were purchased from BD Pharmingen (San Diego, CA, USA). SDS-PAGE gel electrophoresis, trypsin, and BCA protein quantitative kits were purchased from Beyotime Company (Shanghai, China). Penicillin/streptomycin was purchased from Gibco (Carlsbad, CA, USA). A tartrate-resistant acid phosphatase (TRAP) staining kit, cathepsin K (CTSK), calcitonin receptor (CTR), nuclear factor of activated-T cells, cytoplasmic 1 (NFATc1), RANKL, OPG, Runx2, alkaline phosphatase (ALP), CaSR, PTHrP, NF-κB, P65, snail, matrix metalloproteinase-9 (MMP9), and GAPDH antibodies were purchased from Abcam (Cambridge, UK). Electrophoresis and transfer buffers were purchased from Bio-Rad (Hercules, CA, USA). An ECL chemiluminescence kit and NC film were purchased from Millipore (Billerica, MA, USA). An alkaline phosphatase kit was purchased from Nanjing Jiancheng Bioengineering Institute (Nanjing, China). CCK-8 was obtained from DODGEN Chemical Technology Company (Shanghai, China). An *in situ* cell death detection kit was purchased from Roche Molecular Biochemicals (Mannheim, Germany).

2.2. Cell Culture. A549 was purchased from the Cell Library of the Chinese Academy of Sciences and cultured in an F-12k medium containing 10% FBS and 100 U/ml penicillin/streptomycin in a 5% CO_2 atmosphere at 37°C. The cell culture medium was changed every 2 days.

2.3. TRAP Staining. Twenty milliliters of fresh peripheral blood of volunteers were aseptically extracted, and the mononuclear cell layer was obtained after centrifugation. Peripheral blood mononuclear cells were seeded into 96-well plates at a density of 1×10^4 cells per well. The cells were treated with α-MEM containing 10% FBS, 100 U/ml of penicillin, 100 μg/ml of streptomycin, 35 ng/ml of macrophage colony-stimulating factor (M-CSF), 40 ng/mL of murine recombinant receptor activator of nuclear factor-κB ligand (RANKL), and different concentrations of APS (0, 50, 100, and 200 mg/L). The cell culture medium was replaced every 2 days until mature OCs were formed. According to the TRAP staining method of Mostafa et al. [16], the cells were stained for 30 min after 12 days of culture, followed by light microscopy, and the TRAP-positive cells were counted. Cells with >3 nuclei and positive for TRAP staining were considered OCs. TRAP + multinucleated cells were counted under 400x magnification in 5 randomly-selected fields of view. After 15 days of intervention, 5 fields were randomly selected from each group under a 400x magnification field of view, and the size of the osteoclastic area was calculated as

the percentage of the entire field of view. The area of TRAP-stained osteoclasts was calculated with Image J software (NIH, Bethesda, MD, USA).

2.4. Alizarin Red Staining. The rat calvarial cells were isolated as OB precursors and cultured using the Orriss method [21]. The experimental cells used were all 2nd-generation cells. The OB precursors were inoculated into 12-well plates and incubated with different concentrations of APS (0, 50, 100, and 200 mg/L) in an osteogenic medium (1 mM β-glycerophosphate and 5 μm L-ascorbic acid 2-phosphate). For alizarin red staining (AS), cells were washed with 4% paraformaldehyde for 30 min and stained with alizarin red solution for 10 min. The morphology of OBs was observed by an inverted phase contrast microscope. Cell mineralization nodule staining was performed with AS. Pictures were taken under a microscope. The area of AS-stained osteoblasts was also calculated with Image J software (NIH).

2.5. Cell Proliferation Assay. A549 cells were seeded in 96-well plates at a density of 5×10^3 cells/well in the presence of different concentrations of APS (0, 50, 100, and 200 mg/L). After incubation for 24, 48, and 72 h, 10 μL of CCK-8 reagent solution was added to the culture medium, and the cultures were incubated for 1 h at 37°C in a humidified chamber with 95% air and 5% CO_2. The absorbance was measured at 450 nm using an 85 Microplate Reader.

2.6. Flow Cytometry Analysis. A549 cells were treated with APS at different concentrations (0, 50, 100, and 200 mg/L) for 24 h, then washed twice with PBS, collected, and resuspended with binding buffer. The cells were stained with Annexin V and propidium iodide for 30 min. Flow cytometry was performed and FlowJo v.7 software was used for data analysis.

2.7. Transwell Migration Assay. A Transwell migratory apparatus (Costar, Corning Costar, Cambridge, MD, USA) was used for the migration assay. Approximately 1×10^5 cells with different treatments in 200 μL of RPMI-1640 medium were placed in the upper chamber and 1 mL of complete RPMI-1640 medium was placed in the lower chamber. After 24 h in culture, cells were fixed in 4% paraformaldehyde methanol for 30 min and then were stained with 0.1% crystal violet in PBS for 30 min. Cells on the upper side of the filters were removed with cotton-tipped swabs and the filters were washed with PBS. Cells on the underside of the filters were viewed and counted under a microscope (Leica, Wetzlar, Germany).

2.8. Establishment of a Stable CaSR-Overexpression Cell Line. Human A549 cells were cultured in RPMI-1640 medium, and the plasmid carrying the CaSR gene and three helper plasmids were transferred into A549 cells by lentivirus infection. The CaSR gene was inserted into the cell genome. GFP-positive cells were selected by flow cytometry. Monoclonal clones were selected to inoculate 96-well plates. Fluorescence microscopy was performed within 2 weeks. Positive clones were transferred to a 6-well plate to expand the culture and appropriate CaSR-overexpressing stable cell lines were selected according to the level of expression. At the same time, cell lines with empty plasmids were constructed and labeled oeCaSR and oeControl. Similarly, the hairpin structure and the nonsense shRNA sequence were designed according to the mRNA sequence of CaSR in GenBank, and the CaSR knockdown and control cell lines were constructed and labeled siCaSR and siControl. The CaSR siRNA (h) sequence was purchased from Santa Cruz Biotechnology (Cat. No. sc-44373; Santa Cruz, CA, USA) and the control siRNA (h) sequence was purchased from Santa Cruz Biotechnology (Cat. No. sc-37007).

2.9. Western Blot. The cell culture medium was removed and washed twice with PBS, and the cells were scraped off. The prechilled cell lysate was added, and the sample was lysed on ice for 30 min. Protein content was determined by the BCA method. Twelve percentage 1D SDS-PAGE gel electrophoresis was carried out. The protein was transferred to a NC membrane. After blocking with 5% skim milk for 1 h at room temperature, the NC membrane was incubated with the corresponding primary antibody at 4°C overnight, and then, the membrane was washed with TBST for 20 min and it was incubated with the secondary antibody for 1 h at room temperature. The membrane was washed for 20 min with TBST and developed with ECL reagents (Engreen, China). GAPDH was used as an internal control and was detected by the GAPDH antibody. Image J software (NIH) for image processing was used to verify the band intensities as a result of a semiquantitative western blot. The software generated peaks according to the band intensities and the expression was compared between samples and controls. The experiment was repeated three times.

2.10. Establishment of a Mouse Model of Bone Metastasis in Lung Adenocarcinoma. A549 cells growing in culture were washed with PBS and harvested by trypsinization. Only suspensions consisting of single cells with >90% viability were used. The A549 cell suspension (2.5×10^5 cells in 10 μL of PBS) was injected into the right lumen bone platform of BALB/c-Nu/Nu mice according to the method of Chanda et al. [22]. Subsequently, 40 mice were divided into 4 groups of 10 each and injected intraperitoneally (100 μL injection) with different concentrations of APS (0, 50, 100, and 200 mg/L) for 4 weeks. Mice were sacrificed after 28 days and the effects of APS on bone metastasis in lung adenocarcinoma were observed.

2.11. MicroCT Assessment. The fixed right hindlimbs of mice were analyzed by microCT (PerkinElmer, Inc., Waltham, MA, USA) image scanning. The scanning protocol was set, as follows: isometric resolution, 9 mm; and X-ray energy, 80 kV and 800 μA. Bone volume (BV), bone trabecular volume fraction (BV/TV), bone trabecular number (Tb. N), and bone trabecular gaps (Tb. SP) were recorded using the resident reconstruction program (SKYSCAN).

2.12. Histologic Analyses. The right hind limbs were removed after the mice were sacrificed and fixed in PBS (pH 7.2) containing 10% formalin for 2 days, followed by decalcification in 14% ethylenediaminetetraacetic acid (EDTA) with constant stirring over 2 weeks. The decalcified bone specimens were then embedded in paraffin and stained with hematoxylin-eosin (H&E) staining for routine pathological examination.

2.13. Terminal Deoxynucleotidyl Transferase-Mediated Nick-End Labeling (TUNEL) Assay. The TUNEL assay was carried out on tumor tissues as a measurement of *in situ* apoptosis. Bone marrow sections (5 μm thick) of the right hind limb were fixed with formalin, and paraffin-embedded specimens were deparaffinized in xylene, rehydrated in graded alcohol, and transferred to PBS. An *in situ* cell death detection kit (Roche, Mannheim, Germany) was used to perform TUNEL staining according to the manufacturer's instructions. Negative controls were obtained for each sample by the omission of incubation with the TUNEL reaction mixture. Sections were viewed under light microscopy and photographs were obtained.

2.14. Statistical Analysis. SPSS 20.0 software was used to analyze the data. Measurement data were expressed as the mean ± standard deviation ($x \pm s$), and a t-test was used for comparison between the two groups. One-way ANOVA was used for comparisons between multiple groups. A $p < 0.05$ was considered statistically significant.

3. Results

3.1. APS Inhibited OCs Differentiation and the Expression of Related Genes In Vitro. We first induced PBMC differentiation into OCs with RANKL and M-CSF. TRAP staining revealed that the presence of RANKL and M-CSF induced PBMC differentiation into multinucleated OCs. To explore the effect of APS on OCs differentiation, we treated PBMCs with RANKL and M-CSF with different concentrations of APS (0, 50, 100, and 200 mg/L). TRAP staining revealed that APS inhibited RANKL-induced OCs formation as compared to controls, and this inhibitory effect was concentration-dependent (Figures 1(a), 1(c), and 1(d)). We further observed the OCs differentiation status at different time points, and OCs formation was significantly inhibited 7 days after 200 mg/L of APS treatment (Figures 1(b), 1(e), and 1(f)).

To further explore the inhibitory effect of APS on RANKL-induced OCs formation, we examined the expression of gene proteins involved in OCs differentiation, including TRAP, CTSK, CTR, and NFATc1. The results of the western blot showed that the expression of OCs formation-associated protein was significantly inhibited compared with controls treated with RANKL, and the inhibitory effect became more pronounced as the APS concentration increased (Figures 1(g) and 1(h)). The results suggested that APS inhibited RANKL-induced OCs differentiation and the expression of related proteins.

3.2. APS Promotes OBs Differentiation and the Expression of Related Genes In Vitro. To further explore the effect of APS on OBs differentiation, murine calvaria cells were treated with different concentrations of APS (0, 50, 100, and 200 mg/L). ALP staining showed APS to promote OBs differentiation and this facilitation was concentration-dependent (Figures 2(a) and 2(b)).

We further examined the effect of APS on the expression of OB-related proteins. Western blot showed that RANKL protein expression in OBs gradually decreased as the APS concentration increased, whereas the expression of OB-specific proteins, including OPG, Runx2, and ALP, gradually increased (Figures 2(c) and 2(d)). The results suggested that APS promoted OBs differentiation and the expression of related genes.

3.3. Effect of APS on Apoptosis, Proliferation, and Invasion in A549 Cells. To determine the effect of APS on A549 cell proliferation, apoptosis, and invasion, we treated A549 cells with different concentrations of APS (0, 50, 100, and 200 mg/L). First, we examined the proliferation of cells at 24, 48, and 72 h. APS inhibited A549 cell proliferation and reduced the cell number. The number of A549 cells decreased as the APS concentration increased (Figures 3(a) and 3(b)). Second, we examined apoptosis by flow cytometry. The results showed that APS increased the percentage of apoptotic cells and a higher APS concentration induced a higher percentage of apoptotic cells (Figures 3(c) and 3(d)). Finally, we examined A549 cell migration and invasion ability using the Transwell assay. APS inhibited A549 cell migration and this inhibitory effect was concentration-dependent (Figures 3(e) and 3(f)).

3.4. Effect of APS on CaSR and Related Protein Expression in A549 Cells. To further explore the mechanism of APS on bone metastasis of A549 cells, we treated A549 cells with different concentrations of APS (0, 50, 100, and 200 mg/L) and detected the expression of CaSR, NF-κB p65, and PTHrP after APS treatment. Western blot showed that the expression of CaSR, PTHrP, and NF-κB p65 gradually decreased after APS treatment (Figures 4(a) and 4(b)). This result showed that APS inhibited CaSR, PTHrP, and NF-κB p65 in a concentration-dependent manner.

In our previous study [12], we showed that *CaSR* of A549 cells positively regulated the expression of NF-κB p65 and PTHrP, and overexpression or knockout of *CaSR* in A549 cells increased or decreased the expression of NF-κB p65 and PTHrP. In this study, *CaSR* in A549 cells was overexpressed and then treated with APS. The result of the western blot showed that the expression of NF-κB p65 and PTHrP was increased after *CaSR* overexpression, while the expression of

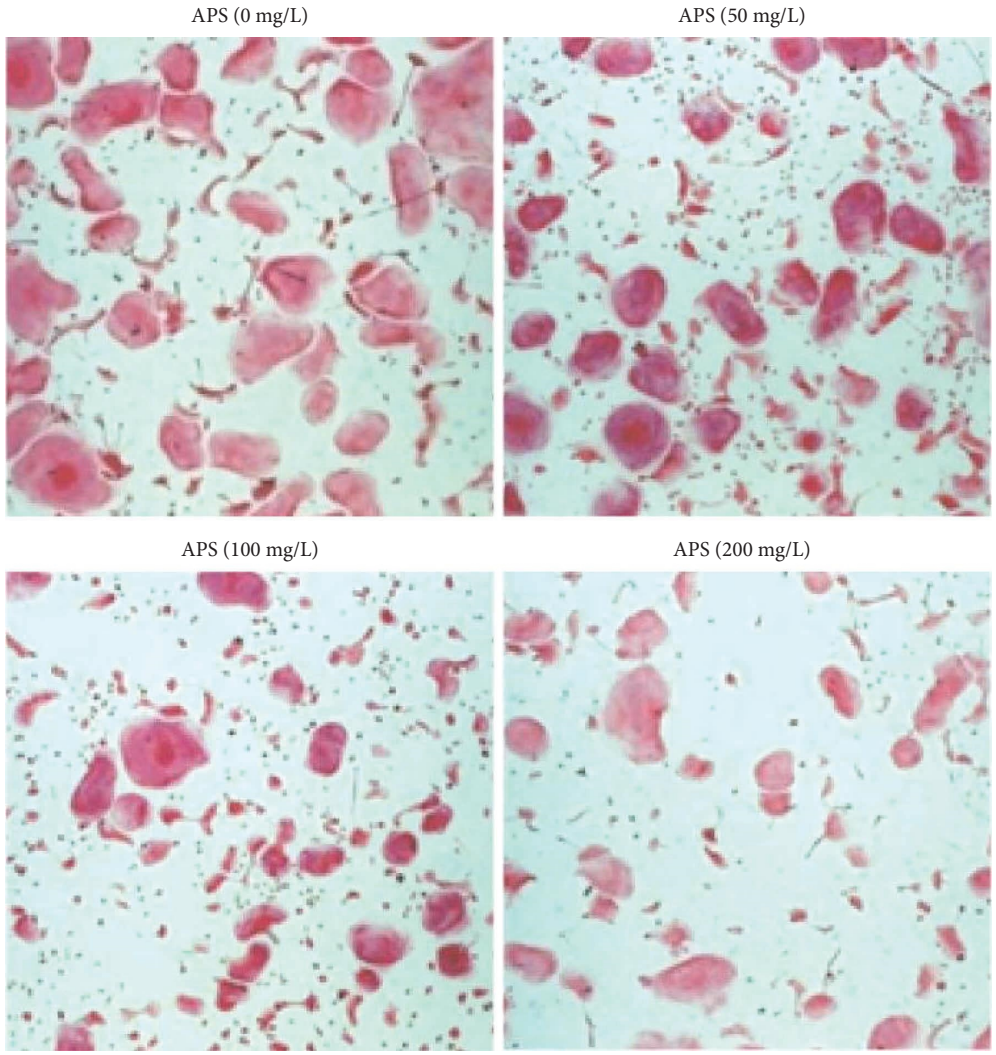

(a)

Figure 1: Continued.

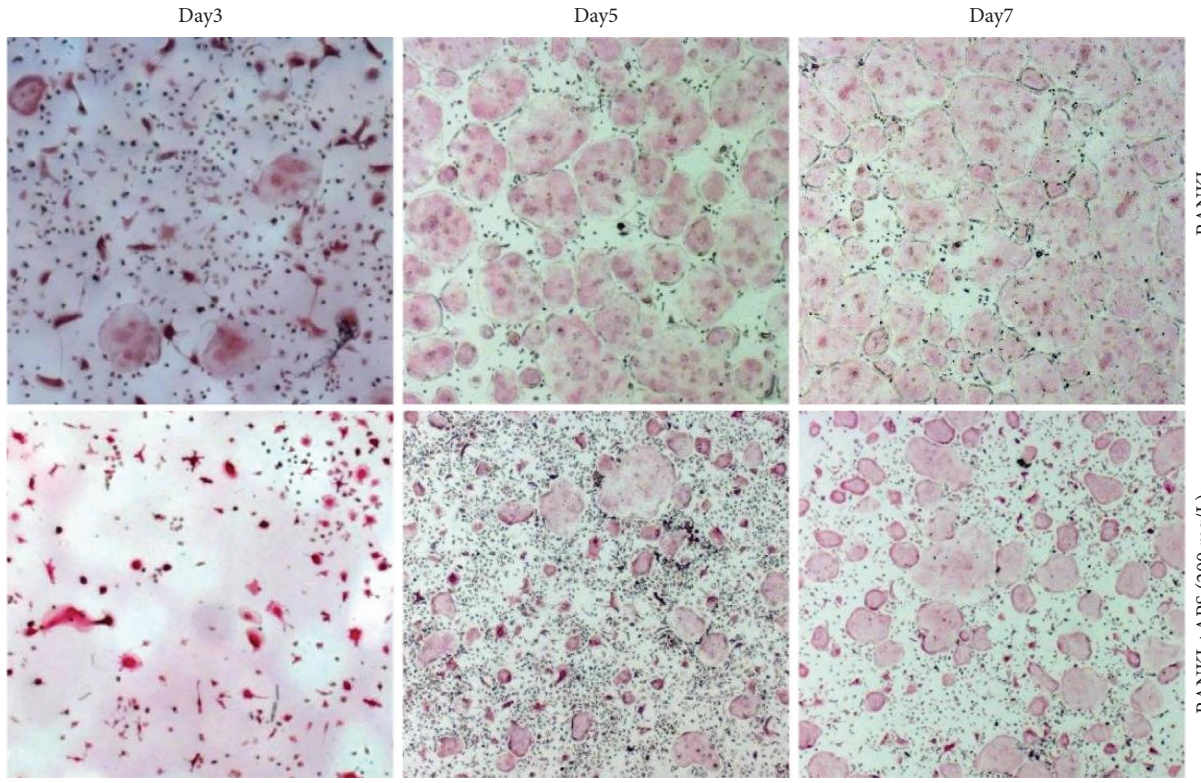

(b)

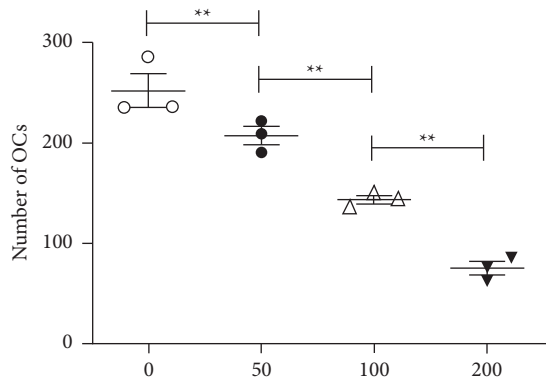

(c)

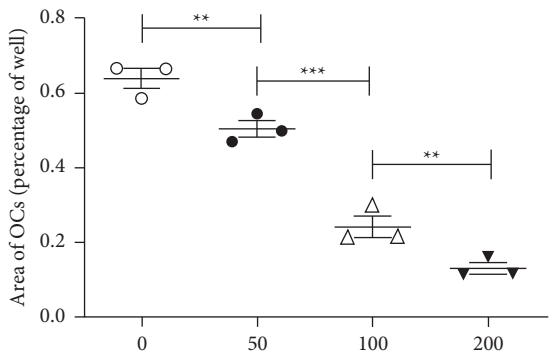

(d)

Figure 1: Continued.

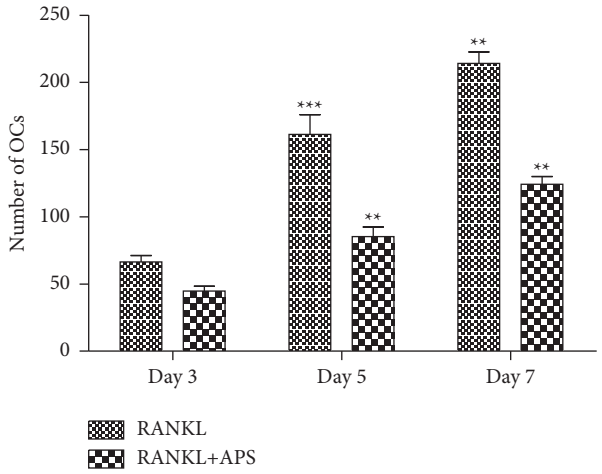

(e)

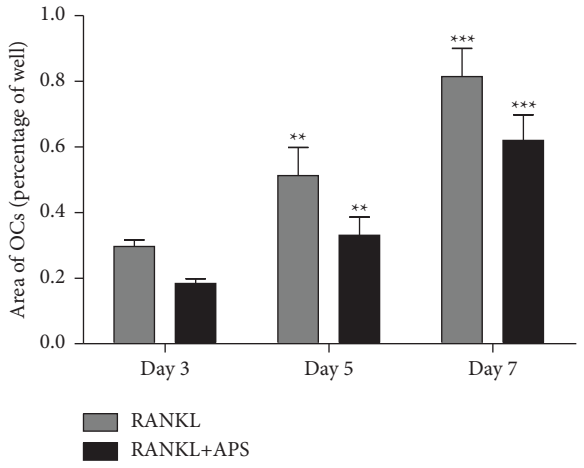

(f)

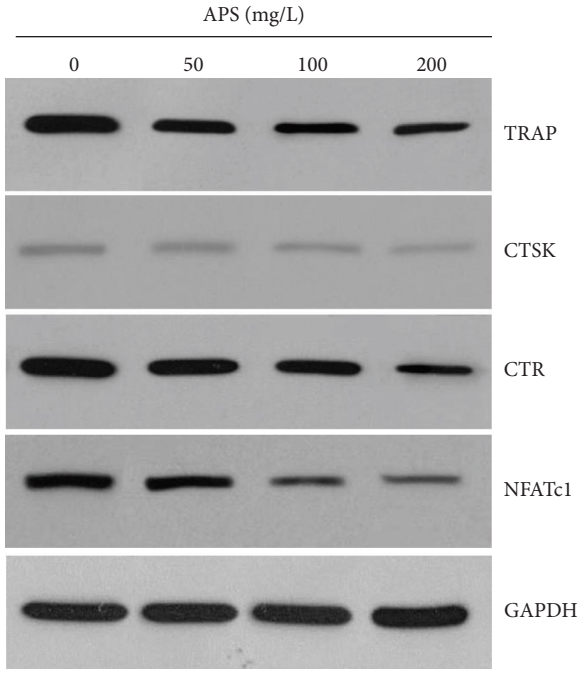

(g)

Figure 1: Continued.

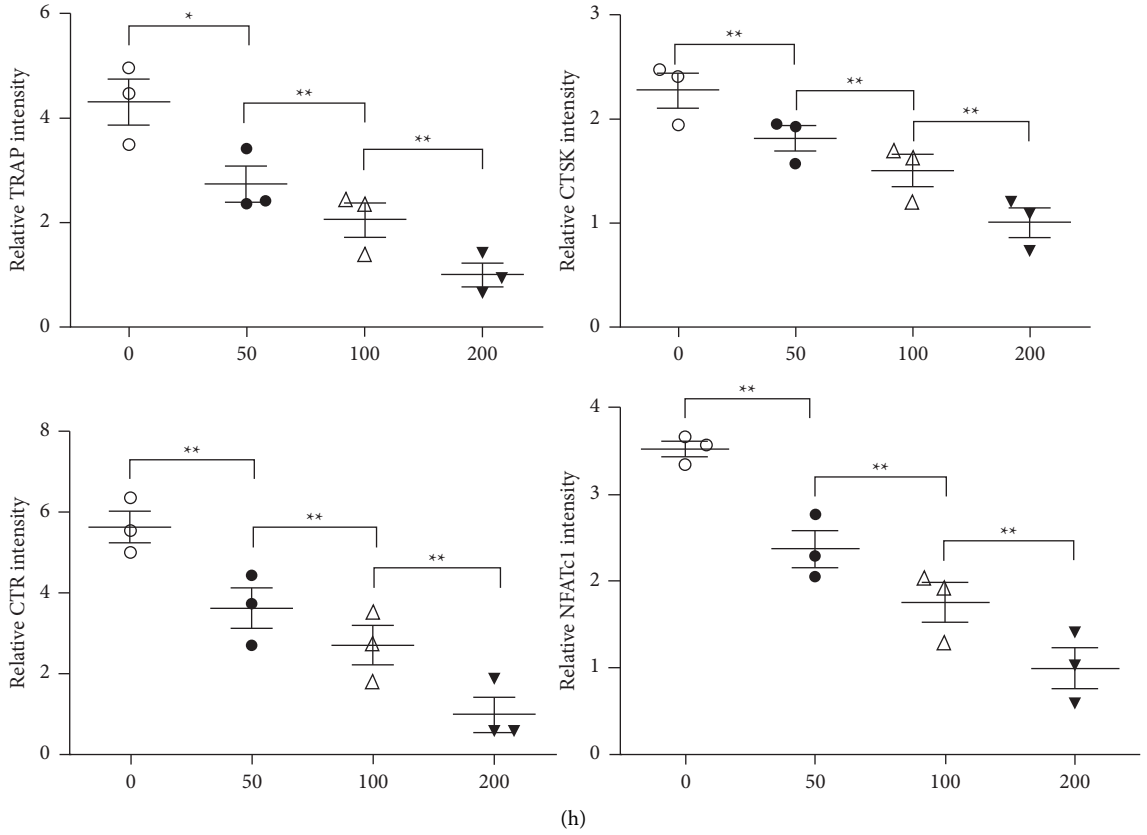

Figure 1: APS inhibited RANKL-induced OCs differentiation and gene expression. (a, c, d) OC precursor cells were treated with different concentrations of APS or cultured for different time points to examine the potential effect on osteoclast differentiation. $TRAP^+$ multinucleated cells were counted under a 400x microscope and the area of TRAP-stained osteoclasts was calculated with Image J software (NIH). The number of OCs and osteolytic area size in the APS-treated group were significantly lower than those of the negative control group ($n = 3$ per group). This inhibitory effect was concentration-dependent. (b, e, f) OCs formation was significantly inhibited 7 days after 200 mg/L of APS treatment according to TRAP staining ($n = 3$ per group). (g, h) The related protein expression of OCs differentiation cathepsin K and CTR, as well as NFATC1 and TRAP, were detected by Western blot after APS treatment. Image J software (NIH) for image processing was used to verify the band intensities as a result of semiquantitative western blots. In the APS treatment group, the protein expression levels of TRAP, cathepsin (K) CTR, and NFATC1 were significantly lower than those of the negative control group ($n = 3$ per group). The inhibitory effect was concentration-dependent. ($^* p < 0.05$, $^{**} p < 0.01$, $^{***} p < 0.001$, $^{****} p < 0.0001$, the statistical test method was one-way ANOVA).

NF-κB p65 and PTHrP decreased after APS treatment. The inhibitory effect was significant between the APS (200 mg/L group) and the negative control group.

3.5. In Vivo Validation of the Effect of APS on Lung Adenocarcinoma Bone Metastasis. To further validate the above conclusions *in vivo*, we constructed a mouse model of A549 cell bone metastasis to validate the effect of APS on lung adenocarcinoma bone metastasis *in vivo*. We treated mice with bone metastases with different concentrations of APS (0, 50, 100, and 200 mg/L). The extent of tumor-induced bone tissue destruction was assessed by microCT and histologic examination. The microCT results showed that APS inhibited bone tissue destruction and increased BV/TV and Tb.N, and reduced Tb.SP. Moreover, this inhibitory effect was concentration-dependent, and the 200 mg/L of APS had a strong inhibitory effect on bone cortical disruption (Figures 5(a)–5(d)). H&E staining observations showed that APS was capable of concentration-dependent inhibition of bone metastatic formation and reducing the degree of infiltration of inflammatory cells (Figure 5(e)).

We further confirmed that APS treatment significantly increased apoptosis in tumor tissues compared to controls based on the TUNEL assay results (Figures 5(f) and 5(g)). All of the above results confirmed that APS inhibited bone metastatic lesions caused by lung adenocarcinoma.

4. Discussion

Advanced lung cancer is the most common malignant tumor in China and worldwide. Bone is the organ most prone to metastasis of advanced lung cancer. Of patients with advanced lung cancer, 30%–40% will have bone metastasis during treatment, and patients with bone metastases will have a shortened survival and poor quality of life. In recent years, drugs such as denosumab and zoledronic acid, have

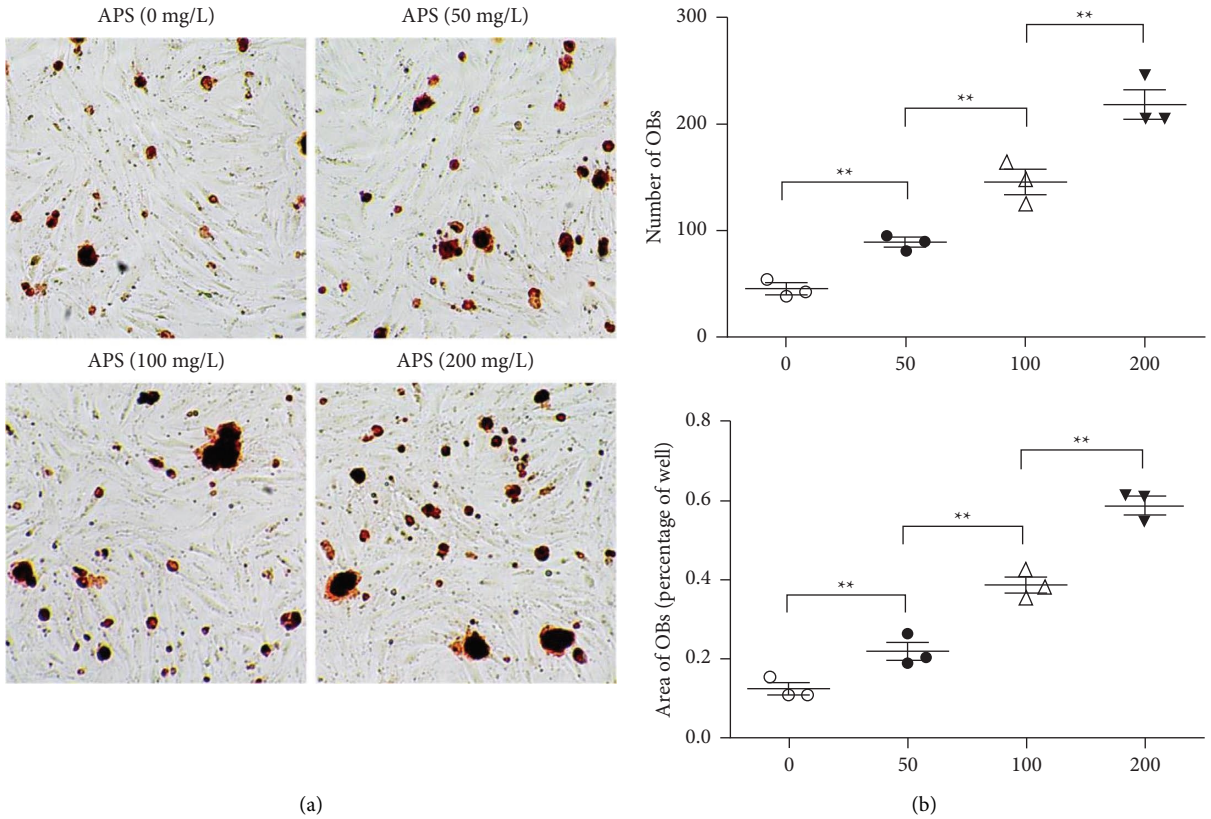

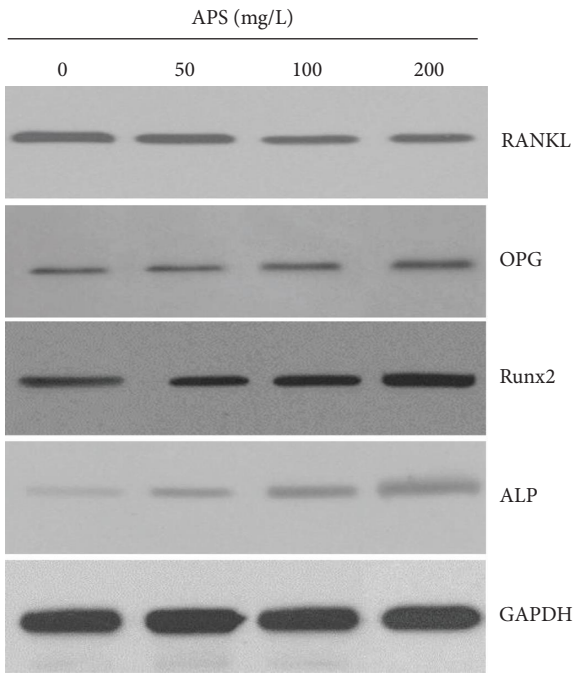

Figure 2: Continued.

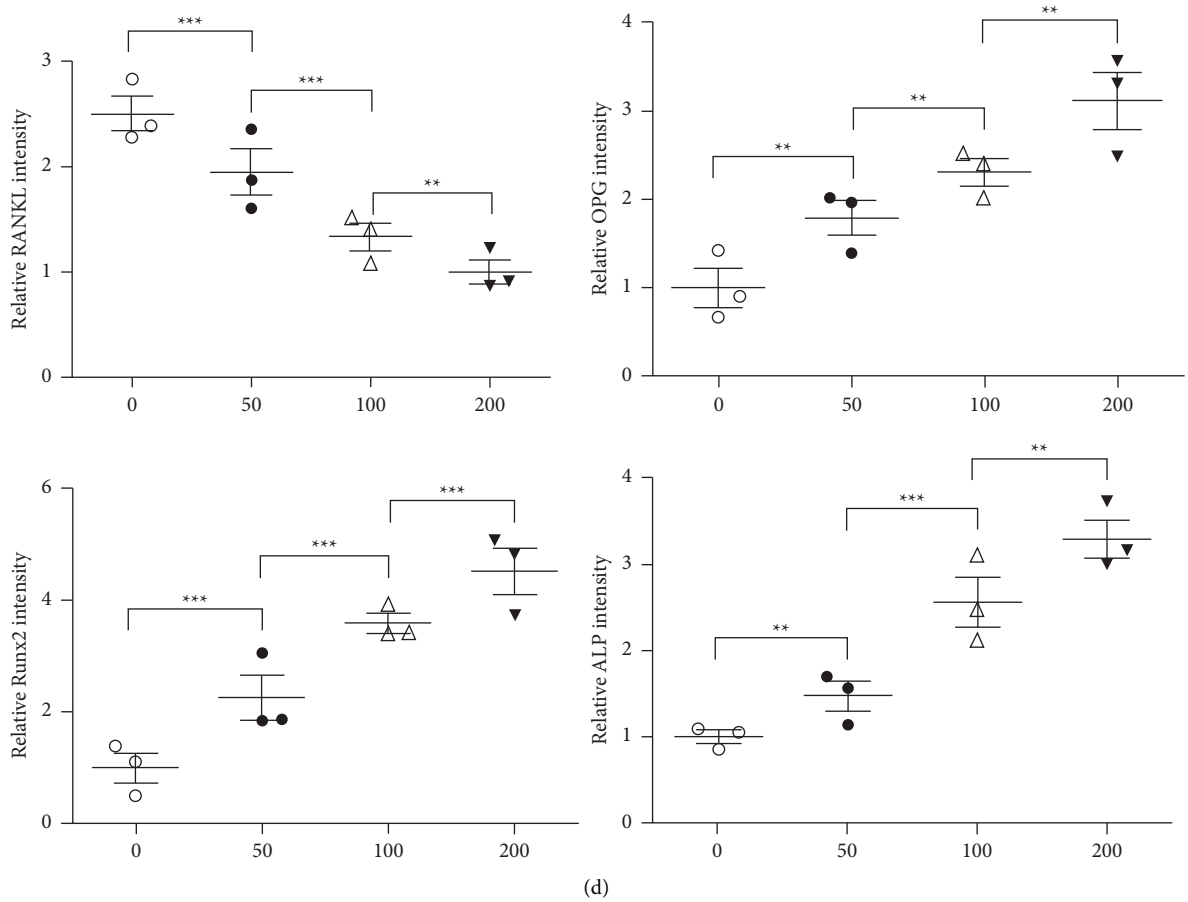

Figure 2: APS promoted OBs differentiation and expression of related genes. (a, b) Osteoblast precursor cells were treated with different concentrations of APS. ALP is a marker for osteoblast activation. ALP staining showed that APS promoted OBs differentiation and this was concentration-dependent ($n = 3$ per group). (c, d) The related protein expression of OBs differentiation RANKL, OPG, Runx2, and ALP was detected by Western blot after APS treatment. Image J software (NIH) for image processing was used to verify the band intensities as a result of semiquantitative western blots. In the APS treatment group, the protein expression of OPG, Runx2, and ALP was significantly higher than those of the negative control group, while RANKL was significantly lower than that of the negative control group ($n = 3$ per group). The effect was concentration-dependent. ($p < 0.05$, $^{**}p < 0.01$, $^{***}p < 0.001$, $^{****}p < 0.0001$, the statistical test method was one-way ANOVA).

been used clinically for the treatment of tumor bone metastases [23–26], reducing the incidence of pathologic fractures, malignant hypercalcemia, and other bone-related events in patients with bone metastases, but the efficacy was limited. Therefore, holistic treatment targeting the interaction between the bone microenvironment and tumor cells may be the key method to improve the curative effect in the future. Traditional Chinese medicine is the treasure of Chinese traditional medicine. Traditional Chinese medicine can improve immune function, regulate the tumor microenvironment, and prevent the occurrence and development of tumors. Traditional Chinese medicine can also act directly on tumor cells and inhibit tumor growth and metastasis. When traditional Chinese medicine is combined with Western medicine, efficacy is increased, toxicity is reduced, and patient survival is prolonged. Astragali Radix is the root of *A. membranaceus* Bunge, which has been widely used in immune response and supports the body to detoxify. Moreover, *A. membranaceus* is considered to be safe and nontoxic, and the dosage of LD50 is approximately 40 g/kg [27]. APS is the main effective constituent of Astragali Radix, which has been widely used in recent years [28]. A number of studies have confirmed that APS could significantly inhibit the migration and invasion of MDA-MB-231 breast cancer cells and H22 liver cancer cells [29, 30]. Other studies have shown that APS had significant antitumor activity in A549 and NCI-H358 human nonsmall cell lung cancer cells [31]. Ou et al. established a mouse model to confirm that APS could promote bone formation by activating the Wnt/LRP5/β-catenin pathway [32]. The preliminary results of this study confirmed that APS could inhibit the differentiation and maturation of OCs and thus disrupt the balance between OBs and OCs, inhibit the proliferation, invasion, and metastasis of lung adenocarcinoma cells, and finally inhibit lung adenocarcinoma bone metastases. The effect may be achieved by intervening in the CaSR/PTHrP pathway of tumor cells.

We first explored the role of APS on OCs and OBs. Indeed, the establishment of tumors requires bone metastasis by bone resorption due to OCs activation, under the

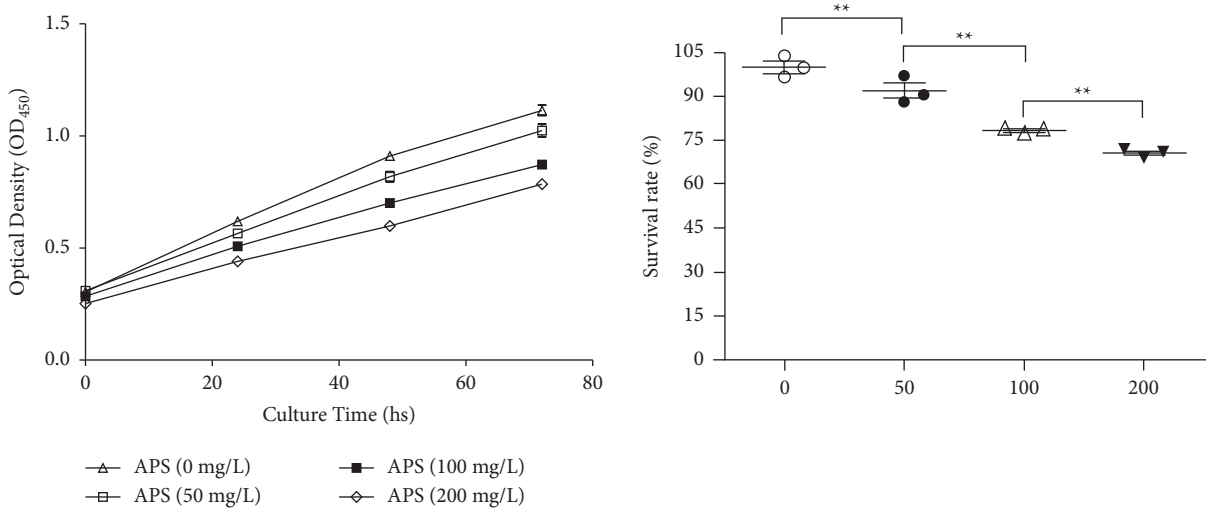

(a)

(b)

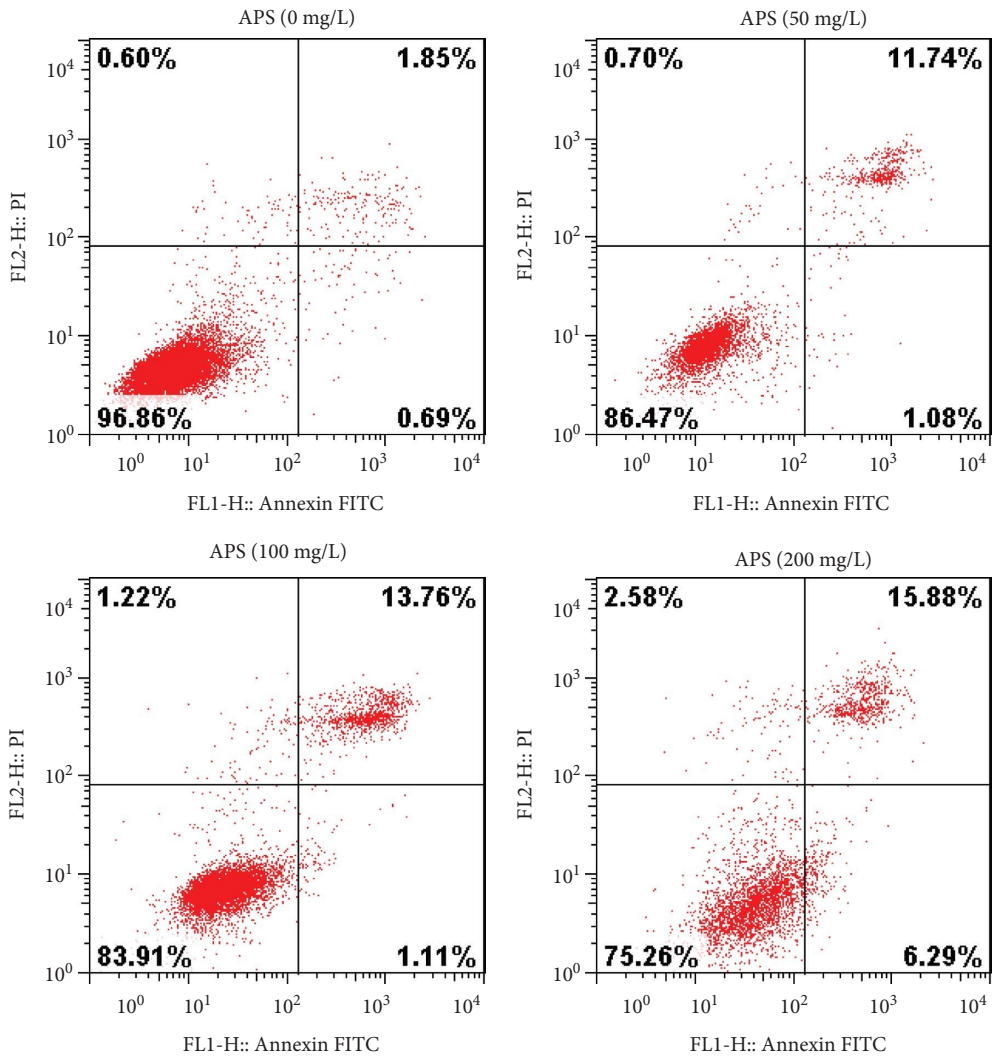

(c)

Figure 3: Continued.

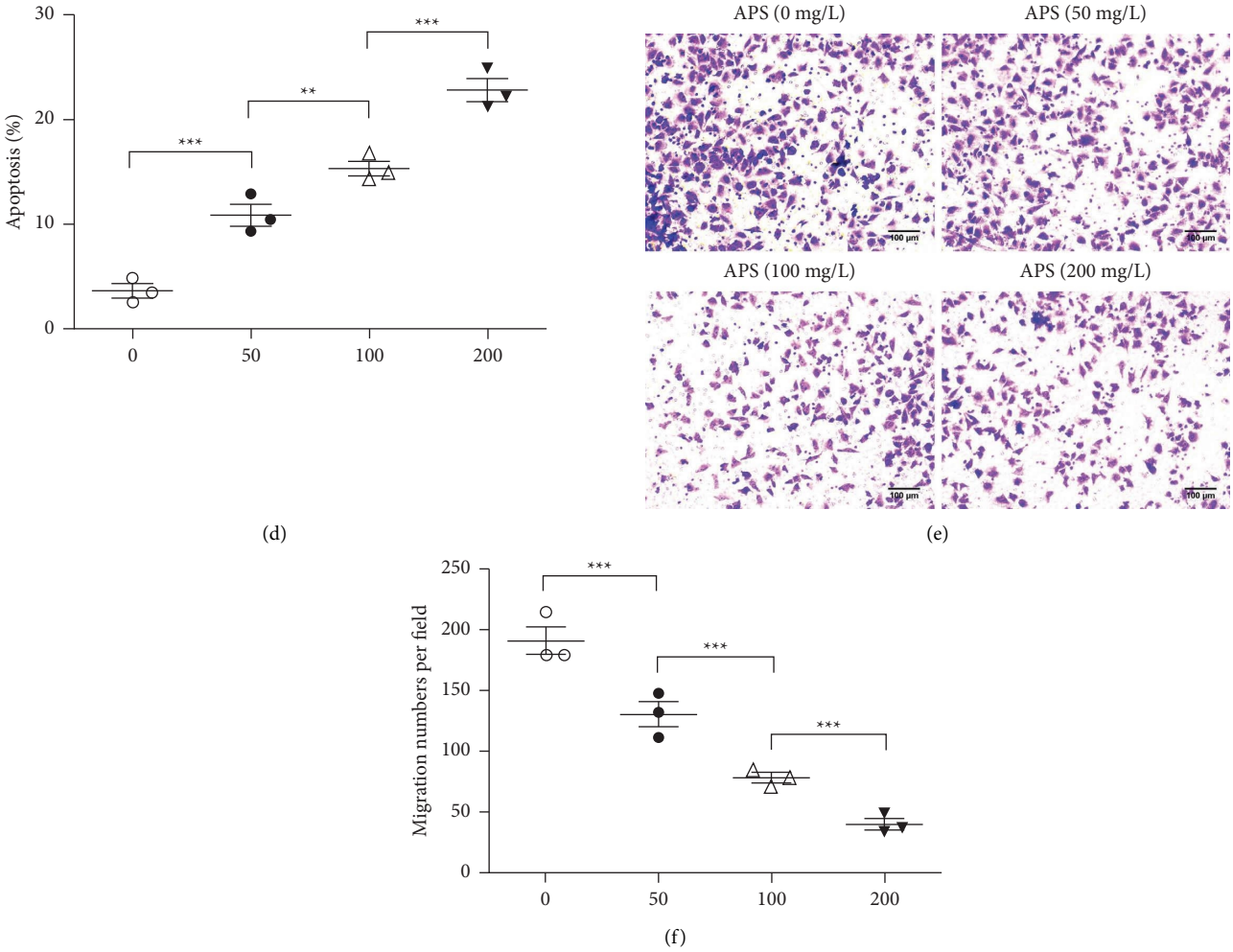

Figure 3: APS promoted A549 cell apoptosis and inhibited A549 cell proliferation and migration. (a, b) CCK-8 was used to detect the proliferation of A549 cells. In the APS-treated group, the proliferation ability of A549 cells was significantly lower than those of the negative control group. The inhibitory effect was concentration-dependent. (c, d) Flow cytometry assay was used to detect cell apoptosis. It showed that APS increased the percentage of apoptotic cells and a higher APS concentration induced a higher percentage of apoptotic cells. (e, f) The cell migration assay showed the effect of APS on migration inhibition in lung adenocarcinoma cells. APS inhibited A549 cell migration and this inhibitory effect was concentration-dependent. ($^{*}p < 0.05$, $^{**}p < 0.01$, $^{***}p < 0.001$, $^{****}p < 0.0001$, the statistical test method was one-way ANOVA).

strict constraints of the bone mineralization structure. OCs maturation leads to the release of CTSK, which creates an acidic environment that promotes bone matrix degradation [33]. TRAP is a characteristic enzyme of OCs and one of the important enzyme histochemical recognition markers of OCs [34]; however, CTR is expressed only in directed OC precursors and mature OCs and is one of the specific identification indicators for OCs [35]. NFATc1 has been shown to be an indispensable regulator of OCs formation and differentiation pathways. Takayanagi et al. reported that embryonic stem cells that specifically knocked out the NFATc1 gene could not successfully differentiate into OCs under the stimulation of RANKL [36]. In addition, NFATc1 also plays an important role in the activation, fusion, and bone resorption function of OCs [37]. Alternatively, as OCs are activated, osteolysis occurs and releases numerous cytokines that act on skeletal stromal cells, activate osteogenesis-associated factors, and promote OBs differentiation [38]. OPG is an induction receptor for RANKL on the surface of OBs that reduces OCs production by binding to RANKL [39]; however, Runt-related transcription factor 2 (Runx2) is a class of specific transcription factors that regulate the differentiation of mesenchymal stem cells (MSCs) towards osteogenesis and are involved in the osteogenesis process [40]. It has been shown that APS improves the balance between OCs and OBs [15]. APS acts as an inhibitor to reduce the activation of MAPK and ROS signaling pathways during OCs genesis associated with RANKL induction, thus suppressing OCs formation due to LPS stimulation [41]. It has also been shown that strontium-based APS promotes OBs differentiation and promotes the proliferation of OBs via the TLR4 signaling pathway, then ossification occurs [42, 43]. In this study, we observed the change in differentiation-related proteins of OC precursors

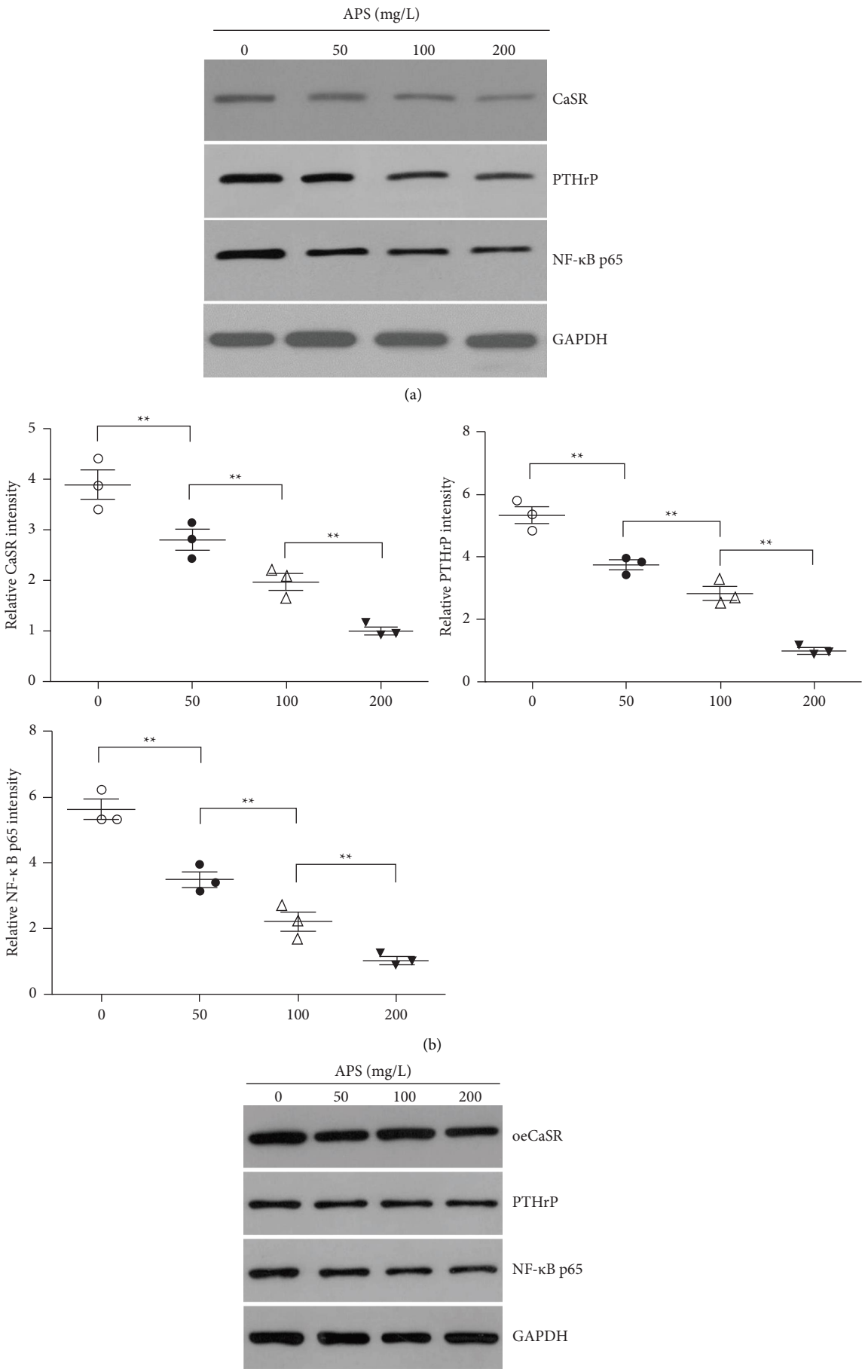

Figure 4: Continued.

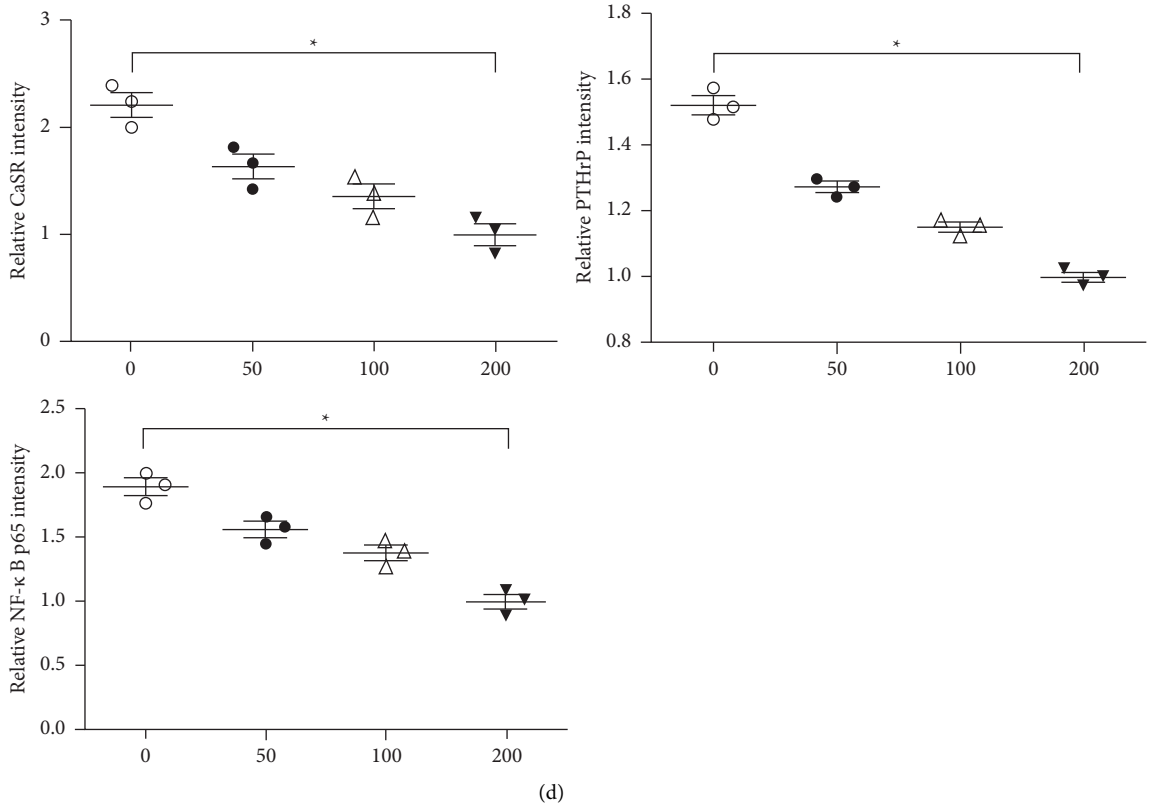

Figure 4: APS inhibited the expression of CaSR-involved signaling pathway-related proteins in A549 cells. (a, b) Western blot confirmed the expression of CaSR, PTHrP, and NF-κB. Image J software (NIH) for image processing was used to verify the band intensities as a result of a semiquantitative western blot. The expressions of CaSR, PTHrP, and NF-κB in the APS-treated group were significantly lower than those of the negative control group. The inhibitory effect was concentration-dependent. (c, d) When CaSR was overexpressed, the expression of PTHrP and NF-κB turned out to be high, while APS inhibited the expression of CaSR, as well as PTHrP and NF-κB ($p < 0.001$). The inhibitory effect was significant between the APS (200 mg/L group) and the negative control group. ($^{*}p < 0.05$, $^{**}p < 0.01$, $^{***}p < 0.001$, $^{****}p < 0.0001$, the statistical test method was one-way ANOVA).

and OBs when treated with different concentrations of APS. The results showed that APS inhibited OCs formation and the expression of its related proteins, and promoted the differentiation of OBs and expression of its related proteins. With an increase in the concentration of APS, the above effect was more apparent. APS was shown to reduce bone tissue destruction by affecting the balance between OCs and OBs. The underlying mechanism may involve CaSR and its downstream-related proteins. The role of APS in the bone microenvironment is expected to provide novel treatments for patients with bone metastasis.

We further explored the effect of APS on tumor cells. Studies have shown that in the process of tumor metastasis, a variety of growth factors and cytokine-binding physical properties provided conditions to promote tumor growth, and extracellular high Ca^{2+} is one of the most important inorganic factors in this process [44]. CaSR widely exists in the parathyroid gland, gastrointestinal tract, kidney, bone, and other tissues and organs that regulate Ca^{2+} homeostasis. Under pathologic conditions, CaSR participates in and regulates the interaction between tumor cells and other intracellular signal molecules, affects cell proliferation and differentiation, and inhibits apoptosis [45]. The effect of CaSR on cancer development may be tissue-specific. Yang et al. believed that there is a correlation between higher calcium intake and lower colorectal cancer risk, and CaSR may play a role in mediating the antitumor effect of calcium [46]. But Binder et al. showed that with the increase of Ca^{2+} content in the diet, the level of CaSR expression was upregulated, which makes prostate tumor cells to have a stronger metastatic ability [47]. In the previous work, our group used A549 cells to construct CaSR overexpression and downregulation of transfected cell lines. After overexpression of CaSR, the proliferation and invasion of A549 cells were significantly enhanced. After downregulating the expression of CaSR, the proliferation and invasion of A549 cells decreased significantly [12]. The results showed that APS significantly inhibited the proliferation and invasion of lung adenocarcinoma cells and promoted their apoptosis.

Many studies have confirmed that CaSR promotes the formation and growth of bone metastasis in prostate, breast, and kidney cancer [48–51]. Mihai et al. confirmed that breast

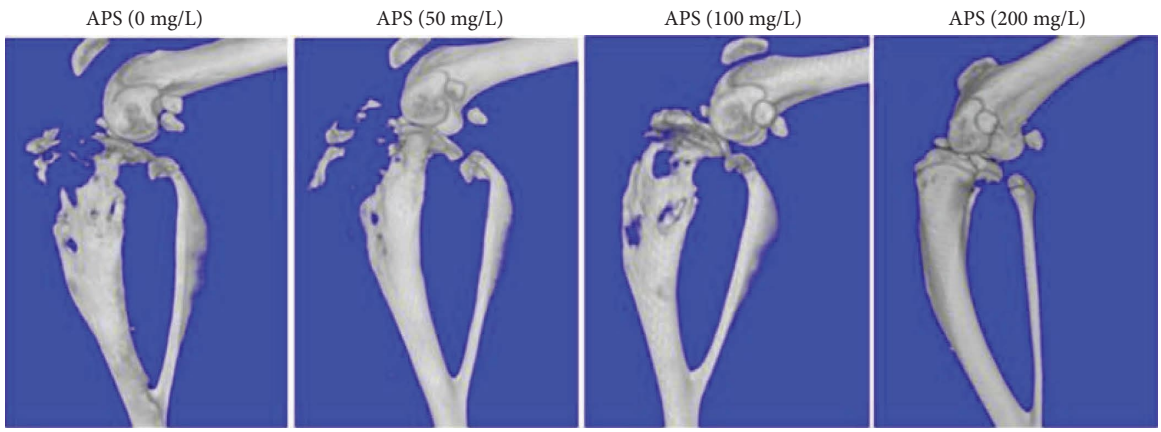

(a)

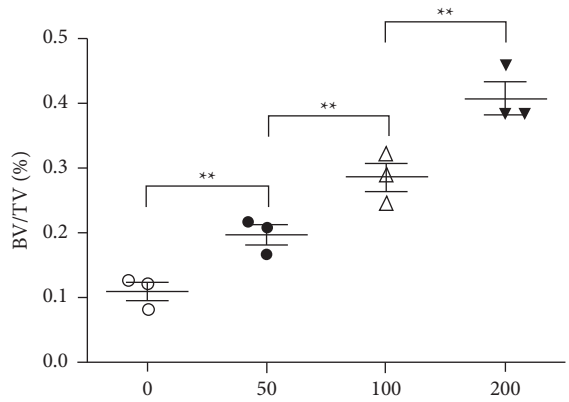

(b)

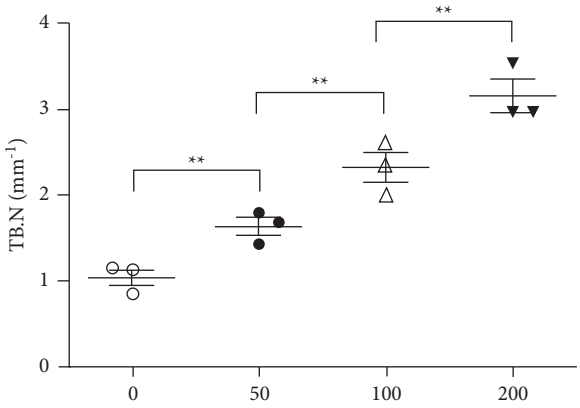

(c)

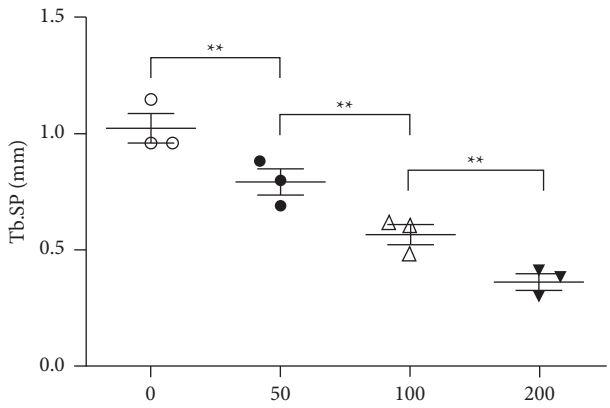

(d)

Figure 5: Continued.

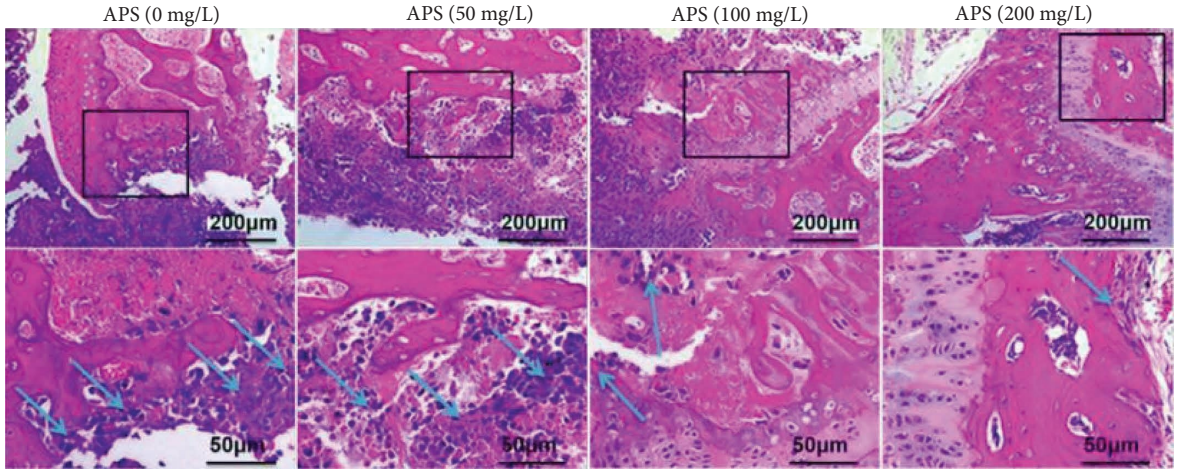

(e)

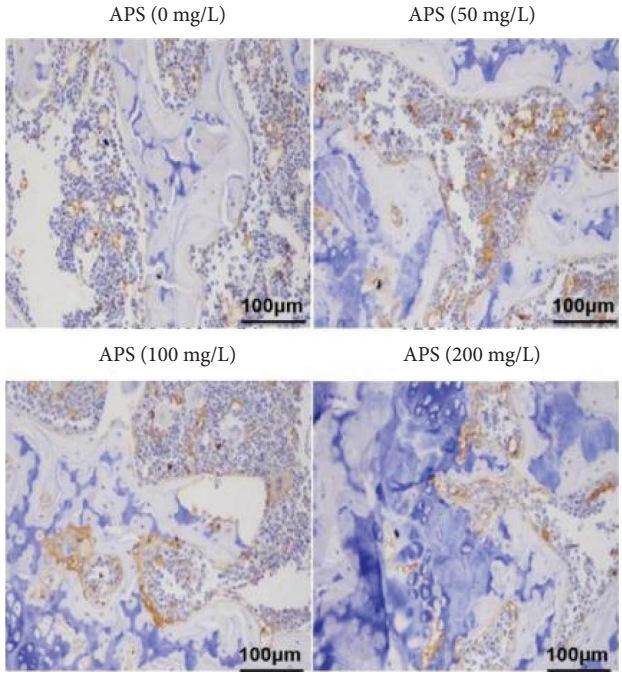

(f)

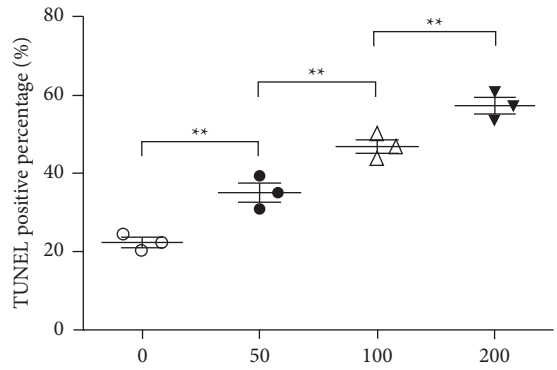

(g)

Figure 5: APS inhibited bone metastasis and osteolysis of lung cancer *in vivo*. (a–d) A549 cells in 10 μL of PBS were injected into the right lumen bone platform of BALB/c-Nu/Nu mice. APS (0, 50, 100, and 200 mg/L) was daily intraperitoneally injected for 4 weeks ($n = 10$ per group; 100 μL injection). Mice were imaged weekly to track tumor progression and the mice were sacrificed at 4 weeks and followed by microCT for the development of the osteolytic lesion area. APS inhibited bone tissue destruction and increased BV/TV and Tb.N, and reduced Tb.SP. This inhibitory effect was concentration-dependent, and the 200 mg/L of APS had a strong inhibitory effect on bone cortical destruction. (e) Representative H&E staining of the hindlimbs is presented. The red arrowheads denote A549 cell infiltration and bone metastasis (f, g). The TUNEL assay was used to detect the effect of APS treatment on A549 cell apoptosis in bone. The TUNEL assay showed that APS treatment promoted apoptosis which was concentration-dependent. ($n = 10$ per group, $^{*}p < 0.05$, $^{**}p < 0.01$, $^{***}p < 0.001$, $^{****}p < 0.0001$, statistical test method was one-way ANOVA).

cancer cells with high CaSR expression had a higher potential for bone metastasis [52]. Feng et al. showed that the expression of CaSR in patients with prostate cancer bone metastases was significantly higher than in patients without bone metastases [53]. When CaSR is upregulated and activated on the surface of tumor cells, CaSR stimulates tumor cells to release PTHrP. PTHrP is produced by tumor cells and induces the expression of RANKL on the surface of OBs and bone stromal cells. RANKL acts on OCs to promote the maturation and absorption activity of OCs and increases the ability of osteolysis. Previous studies have shown that PTHrP is an important regulatory factor of bone metastasis and

promotes tumor growth and progression of bone metastasis with growth factors, such as TGF-β and chemokine C-C motif ligand 2 (CCL2) [54, 55]. In the bone microenvironment, the production of PTHrP stimulates osteoclastic bone resorption, which leads to the release of active TGF-β [56]. TGF-β acts on tumor cells again, promotes the metastatic ability, and stimulates the production of PTHrP [56]. Therefore, PTHrP is an important effector in the process of bone metastasis. In contrast, NF-κB is an important intracellular transcription factor. NF-κB plays a key role in tumor occurrence, development, and metastasis [57]. Our previous results suggested that CaSR promoted the expression of NF-κB p65 and PTHrP, which is closely related to bone metastasis of lung adenocarcinoma [12]. Several studies have shown that APS inhibits the activation of MAPK and ROS signaling pathways during OCs differentiation associated with RANKL induction, and APS inhibits the production of inflammatory factors and chemokines by inhibiting activation of the MAPK and NF-κB inflammatory pathways [41]. In this study, we found that APS not only inhibited the expression of CaSR in lung adenocarcinoma A549 cells but also inhibited the expression of PTHrP and NF-κB p65 induced by CaSR overexpression. The inhibitory effect of APS (200 mg/L group) was significantly different from the negative control group. The results suggested that APS may inhibit the expression of PTHrP and NF-κB p65 regulation by CaSR and ultimately inhibit the proliferation, invasion, and bone metastasis of lung adenocarcinoma cells.

Finally, we constructed a mouse model of A549 cell bone metastasis to further verify the effect of APS on bone metastasis and osteolysis of lung adenocarcinoma. The evaluation parameters of bone tissue mainly include BV, BV/TV, Tb.N, and Tb.Sp. These parameters are bone analysis parameters calculated based on CT images, which can evaluate the condition of the bone. The results showed that APS increased BV/TV and Tb.N, decreased Tb.Sp, and inhibited bone destruction. HE staining directly indicates cancer cell infiltration. We found that APS significantly inhibited the infiltration of A549 cells into bone. The TUNEL assay further suggested that APS promoted apoptosis of A549 cells. These results indirectly verified the inhibitory effect of APS on bone metastasis because A549 cells can overexpress CaSR, thereby promoting the secretion of PTHrP by cancer cells, then activating OCs to initiate osteolytic damage. The *in vivo* experiments in mice showed that APS might inhibit bone metastasis by alleviating bone destruction and promoting apoptosis of cancer. In our previous study, it was confirmed that CaSR and PTHrP could affect the differentiation of OCs and OBs. More interestingly, it was indicated in this study that APS may inhibit OCs and OBs differentiation through CaSR/PTHrP pathway *in vitro*. Besides OCs and OBs, osteocytes, bone lining cells, osteomas, and vascular endothelial cells also regulate bone remodeling [58]. Studies have reported the effects of APS on osteocytes and vascular endothelial cells in bone [59]. It has been found that APS can promote angiogenesis and osteocyte proliferation in the coculture system of endothelial cells and primary human OBs through the MyD88-dependent TLR4 signaling pathway *in vitro* [60]. However, we have not found any studies exploring the relationship between APS and bone lining cells and osteomas. This study was a preliminary attempt to explore the protective effect of APS on bone metastasis of lung adenocarcinoma. Much more work should be undertaken to confirm our conclusion in future.

5. Conclusions

APS may inhibit the proliferation and invasion of lung adenocarcinoma cells by inhibiting the expression of CaSR and its related regulatory proteins PTHrP and NF-κB p65 and also inhibit the proliferation and invasion of lung adenocarcinoma cells and affect the balance of OCs and OBs in the bone microenvironment and thus have a certain protective effect on bone metastasis of [61] lung adenocarcinoma.

Abbreviations

OC: Osteoclast
OB: Osteoblast
Ca^{2+}: Calcium ion
CaSR: Calcium sensing receptor
EMT: Epithelial-mesenchymal transition
PTHrP: Parathyroid hormone-related protein
RANKL: Receptor activator of nuclear factor-κB ligand
NF-κB: Kappa-light-chain enhancer of activated B cells
APS: *Astragalus* polysaccharide
M-CSF: Macrophage colony-stimulating factor
TRAP: Tartrate-resistant acid phosphatase
CTSK: Cathepsin K
CTR: Calcitonin receptor
NFATc1: Nuclear factor of activated-T cells, cytoplasmic 1
ALP: Alkaline phosphatase
MMP: Matrix metalloproteinase
PBMC: Peripheral blood mononuclear cell
BV: Bone volume
BV/TV: Bone trabecular volume fraction
Tb. N: Bone trabecular number
Tb. SP: Bone trabecular gaps
HE: Hematoxylin-eosin
TUNEL: TdT-mediated dUTP nick-end labeling
Runx2: Runt-related transcription factor 2
MSC: Mesenchymal stem cell.

Data Availability

The data used to support the findings of this study have not been made available.

Additional Points

Practical Applications. *Astragalus* polysaccharide has antitumor activity and alleviates osteoporosis. In this study, we confirmed that APS inhibits the proliferation and invasion of

lung adenocarcinoma cells *in vivo* and *in vitro* by inhibiting the expression of CaSR and its related regulatory proteins, PTHrP and NF-κB p65, and affects the balance of OCs and OBs in the bone microenvironment, thus having a protective effect on bone metastasis of lung adenocarcinoma.

Ethical Approval

All animal experiments were performed in accordance with guidelines for animal treatment of Beijing Friendship Hospital, Capital Medical University. All experimental protocols in this study were approved by the Ethics Committee of Beijing Friendship Hospital, Capital Medical University.

Consent

Not applicable.

Conflicts of Interest

The authors declare that they have no conflicts of interests and all the authors confirm that the study is reported in accordance with ARRIVE guidelines.

Authors' Contributions

Xiaoting Ma and Cong Wang contributed equally to this work. XTM and JY conceptualized and designed this study. XTM and CW carried out the experiments, wrote the manuscript, and approved the final submission of the study. JY provided the funds. All authors read and approved the final manuscript.

Acknowledgments

This work was supported by the National Natural Science Foundation of China (Grant no. 81774221) and Beijing Natural Science Foundation of China (No. 7212168).

Supplementary Materials

CaSR Protein Expression. Western blot was used to verify the level of CaSR expression after cell line *construction*. In the CaSR overexpression group, the level of CaSR protein expression in A549 cells was significantly higher than those of the negative control group ($p < 0.001$). (*Supplementary Materials*)

References

[1] The Lancet, "Lung cancer: some progress, but still a lot more to do," *The Lancet*, vol. 394, no. 10212, p. 1880, 2019.

[2] E. Akoury, A. S. Ramirez Garcia Luna, P. Ahangar et al., "Anti-tumor effects of low dose zoledronate on lung cancer-induced spine metastasis," *Journal of Clinical Medicine*, vol. 8, no. 8, p. 1212, 2019.

[3] Y. Y. Chen, P. P. Wang, Y. Fu et al., "Inferior outcome of bone metastasis in non-small-cell-lung-cancer patients treated with epidermal growth factor receptor inhibitors," *Journal of Bone Oncology*, vol. 29, Article ID 100369, 2021.

[4] L. Zhang and Z. Gong, "Clinical characteristics and prognostic factors in bone metastases from lung cancer," *Medical Science Monitor*, vol. 23, pp. 4087–4094, 2017.

[5] A. Tuffour, A. A. Kosiba, Y. Zhang, F. A. Peprah, J. Gu, and H. Shi, "Role of the calcium-sensing receptor (CaSR) in cancer metastasis to bone: identifying a potential therapeutic target," *Biochimica et Biophysica Acta (BBA) - Reviews on Cancer*, vol. 1875, no. 2, Article ID 188528, 2021.

[6] I. Breuksch, M. Weinert, and W. Brenner, "The role of extracellular calcium in bone metastasis," *Journal of Bone Oncology*, vol. 5, no. 3, pp. 143–145, 2016.

[7] D. T. Ward and D. Riccardi, "New concepts in calcium-sensing receptor pharmacology and signalling," *British Journal of Pharmacology*, vol. 165, no. 1, pp. 35–48, 2012.

[8] S. Tennakoon, A. Aggarwal, and E. Kállay, "The calcium-sensing receptor and the hallmarks of cancer," *Biochimica et Biophysica Acta (BBA) - Molecular Cell Research*, vol. 1863, no. 6, pp. 1398–1407, 2016.

[9] I. Breuksch, M. Weinert, and W. Brenner, "The role of extracellular calcium in bone metastasis," *Journal of Bone Oncology*, vol. 5, no. 3, pp. 143–145, 2016.

[10] P. L. Kuo, S. H. Liao, J. Y. Hung, M. S. Huang, and Y. L. Hsu, "MicroRNA-33a functions as a bone metastasis suppressor in lung cancer by targeting parathyroid hormone related protein," *Biochimica et Biophysica Acta (BBA) - General Subjects*, vol. 1830, no. 6, pp. 3756–3766, 2013.

[11] W. Kim, F. M. Takyar, K. Swan et al., "Calcium-sensing receptor promotes breast cancer by stimulating intracrine actions of parathyroid hormone-related protein," *Cancer Research*, vol. 76, no. 18, pp. 5348–5360, 2016.

[12] L. Liu, Y. Fan, Z. Chen, Y. Zhang, and J. Yu, "CaSR induces osteoclast differentiation and promotes bone metastasis in lung adenocarcinoma," *Frontiers in Oncology*, vol. 10, p. 305, 2020.

[13] H. Ming, Y. Chen, F. Zhang et al., "[Astragalus polysaccharides combined with cisplatin decreases the serum levels of CD44 and collagen type IV and hyaluronic acid in mice bearing Lewis lung cancer]," *Xi Bao Yu Fen Zi Mian Yi Xue Za Zhi*, vol. 31, no. 7, pp. 909–913, 2015, [Chinese].

[14] M. McCulloch, C. See, X. J. Shu et al., "Astragalus-based Chinese herbs and platinum-based chemotherapy for advanced non-small-cell lung cancer: meta-analysis of randomized trials," *Journal of Clinical Oncology*, vol. 24, no. 3, pp. 419–430, 2006.

[15] J. Liu, J. Liu, S. Duan, L. Liu, G. Zhang, and X. Peng, "Reprogrammed epigenetic landscape-prophesied functions of bioactive polysaccharides in alleviating diseases: a pilot study of dna methylome remodeling in Astragalus polysaccharide (APS)-Improved osteoporosis in a rat model," *Journal of Agricultural and Food Chemistry*, vol. 68, no. 52, pp. 15449–15459, 2020.

[16] Y. P. Zhu, T. Shen, Y. J. Lin et al., "Astragalus polysaccharides suppress ICAM-1 and VCAM-1 expression in TNF-α-treated human vascular endothelial cells by blocking NF-κB activation," *Acta Pharmacologica Sinica*, vol. 34, no. 8, pp. 1036–1042, 2013.

[17] J. Lv, Y. Zhang, Z. Tian et al., "Astragalus polysaccharides protect against dextran sulfate sodium-induced colitis by inhibiting NF-κB activation," *International Journal of Biological Macromolecules*, vol. 98, pp. 723–729, 2017.

[18] J. Gallardo-Pã©rez, M. Espinosa, G. Ceballos-Cancino et al., "NF-kappa B is required for the development of tumor spheroids," *Journal of Cellular Biochemistry*, vol. 108, no. 1, pp. 169–180, 2009.

[19] Y. Zhou, T. Hong, L. Tong et al., "Astragalus polysaccharide combined with 10-hydroxycamptothecin inhibits metastasis in non-small cell lung carcinoma cell lines via the MAP4K3/mTOR signaling pathway," *International Journal of Molecular Medicine*, vol. 42, no. 6, pp. 3093–3104, 2018.

[20] O. A. Bamodu, K. T. Kuo, C. H. Wang et al., "Astragalus polysaccharides (PG2) enhances the M1 polarization of macrophages, functional maturation of dendritic cells, and T cell-mediated anticancer immune responses in patients with lung cancer," *Nutrients*, vol. 11, no. 10, p. 2264, 2019.

[21] I. R. Orriss, S. E. B. Taylor, and T. R. Arnett, "Rat osteoblast cultures," *Methods in Molecular Biology*, vol. 816, pp. 31–41, 2012.

[22] D. Chanda, S. Kumar, and S. Ponnazhagan, "Therapeutic potential of adult bone marrow-derived mesenchymal stem cells in diseases of the skeleton," *Journal of Cellular Biochemistry*, vol. 111, no. 2, pp. 249–257, 2010.

[23] S. A. Eccles and D. R. Welch, "Metastasis: recent discoveries and novel treatment strategies," *The Lancet*, vol. 369, no. 9574, pp. 1742–1757, 2007.

[24] J. Y. Krzeszinski and Y. Wan, "New therapeutic targets for cancer bone metastasis," *Trends in Pharmacological Sciences*, vol. 36, no. 6, pp. 360–373, 2015.

[25] D. L. Lacey, W. J. Boyle, W. S. Simonet et al., "Bench to bedside: elucidation of the OPG-RANK-RANKL pathway and the development of denosumab," *Nature Reviews Drug Discovery*, vol. 11, no. 5, pp. 401–419, 2012.

[26] R. E. Coleman, "Prevention and treatment of bone metastases," *Nature Reviews Clinical Oncology*, vol. 9, no. 2, pp. 76–78, 2011.

[27] A. Sheik, K. Kim, G. L. Varaprasad et al., "The anti-cancerous activity of adaptogenic herb Astragalus membranaceus," *Phytomedicine*, vol. 91, Article ID 153698, 2021.

[28] N. Ye, J. Cruz, X. Peng, J. Ma, A. Zhang, and X. Cheng, "Remyelination is enhanced by Astragalus polysaccharides through inducing the differentiation of oligodendrocytes from neural stem cells in cuprizone model of demyelination," *Brain Research*, vol. 1763, Article ID 147459, 2021.

[29] S. Yang, S. Sun, W. Xu, B. Yu, G. Wang, and H. Wang, "Astragalus polysaccharide inhibits breast cancer cell migration and invasion by regulating epithelial-mesenchymal transition via the Wnt/β-catenin signaling pathway," *Molecular Medicine Reports*, vol. 21, no. 4, pp. 1819–1832, 2020.

[30] W. H. Huang, W. R. Liao, and R. X. Sun, "Astragalus polysaccharide induces the apoptosis of human hepatocellular carcinoma cells by decreasing the expression of Notch1," *International Journal of Molecular Medicine*, vol. 38, no. 2, pp. 551–557, 2016.

[31] C. Y. Wu, Y. Ke, Y. F. Zeng, Y. W. Zhang, and H. J. Yu, "Anticancer activity of Astragalus polysaccharide in human non-small cell lung cancer cells," *Cancer Cell International*, vol. 17, no. 1, p. 115, 2017.

[32] L. Ou, P. Wei, M. Li, and F. Gao, "Inhibitory effect of Astragalus polysaccharide on osteoporosis in ovariectomized rats by regulating FoxO3a/Wnt signaling pathway," *Acta Cirurgica Brasileira*, vol. 34, no. 5, Article ID e201900502, 2019.

[33] A. S. Gdowski, A. Ranjan, and J. K. Vishwanatha, "Current concepts in bone metastasis, contemporary therapeutic strategies and ongoing clinical trials," *Journal of Experimental & Clinical Cancer Research*, vol. 36, no. 1, p. 108, 2017.

[34] K. Henriksen, J. Gram, S. Schaller et al., "Characterization of osteoclasts from patients harboring a G215R mutation in ClC-7 causing autosomal dominant osteopetrosis type II," *American Journal Of Pathology*, vol. 164, no. 5, pp. 1537–1545, 2004.

[35] J. M. Quinn, M. Morfis, M. H. Lam et al., "Calcitonin receptor antibodies in the identification of osteoclasts," *Bone*, vol. 25, no. 1, pp. 1–8, 1999.

[36] H. Takayanagi, S. Kim, T. Koga et al., "Induction and activation of the transcription factor NFATc1 (NFAT2) integrate RANKL signaling in terminal differentiation of osteoclasts," *Developmental Cell*, vol. 3, no. 6, pp. 889–901, 2002.

[37] J. H. Park, N. K. Lee, and S. Y. Lee, "Current understanding of RANK signaling in osteoclast differentiation and maturation," *Molecules and Cells*, vol. 40, no. 10, pp. 706–713, 2017.

[38] A. Schmid-Alliana, H. Schmid-Antomarchi, R. Al-Sahlanee, P. Lagadec, J. C. Scimeca, and E. Verron, "Understanding the progression of bone metastases to identify novel therapeutic targets," *International Journal of Molecular Sciences*, vol. 19, no. 1, p. 148, 2018.

[39] N. Udagawa, M. Koide, M. Nakamura et al., "Osteoclast differentiation by RANKL and OPG signaling pathways," *Journal of Bone and Mineral Metabolism*, vol. 39, no. 1, pp. 19–26, 2021.

[40] K. Gomathi, N. Akshaya, N. Srinaath, A. Moorthi, and N. Selvamurugan, "Regulation of Runx2 by post-translational modifications in osteoblast differentiation," *Life Sciences*, vol. 245, Article ID 117389, 2020.

[41] J. Yang, L. Qin, J. Huang et al., "Astragalus polysaccharide attenuates LPS-related inflammatory osteolysis by suppressing osteoclastogenesis by reducing the MAPK signalling pathway," *Journal of Cellular and Molecular Medicine*, vol. 25, no. 14, pp. 6800–6814, 2021.

[42] Y. Peng, F. Ma, L. Hu, Y. Deng, W. He, and B. Tang, "Strontium based Astragalus polysaccharides promote osteoblasts differentiation and mineralization," *International Journal of Biological Macromolecules*, vol. 205, pp. 761–771, 2022.

[43] H. Qiu, L. Zhang, X. He et al., "Promotion of angiogenesis in vitro by Astragalus polysaccharide via activation of TLR4 signaling pathway," *Journal of Food Biochemistry*, vol. 46, no. 10, Article ID e14329, 2022.

[44] A. T. Manning, N. O'Brien, and M. J. Kerin, "Roles for the calcium sensing receptor in primary and metastatic cancer," *European Journal of Surgical Oncology*, vol. 32, no. 7, pp. 693–697, 2006.

[45] C. Vahe, K. Benomar, S. Espiard et al., "Diseases associated with calcium-sensing receptor," *Orphanet Journal of Rare Diseases*, vol. 12, no. 1, p. 19, 2017.

[46] W. Yang, L. Liu, Y. Masugi et al., "Calcium intake and risk of colorectal cancer according to expression status of calcium-sensing receptor (CASR)," *Gut*, vol. 67, no. 8, pp. 1475–1483, 2018.

[47] M. Binder, I. M. Shui, K. M. Shui, K. L. Wilson, and A. S PenneyMucci, "Calcium intake, polymorphisms of the calcium-sensing receptor, and recurrent/aggressive prostate cancer," *Cancer Causes & Control*, vol. 26, no. 12, pp. 1751–1759, 2015.

[48] T. Yamaguchi, "The calcium-sensing receptor in bone," *Journal of Bone and Mineral Metabolism*, vol. 26, no. 4, pp. 301–311, 2008.

[49] V. R. Yadav, T. Song, L. Mei, L. Joseph, Y. M. Zheng, and Y. X. Wang, "PLCγ1-PKCε-IP3R1 signaling plays an important role in hypoxia-induced calcium response in pulmonary artery smooth muscle cells," *American Journal of Physiology - Lung Cellular and Molecular Physiology*, vol. 314, no. 5, pp. L724–L735, 2018.

[50] J. Feng, X. Xu, B. Li et al., "Prostate cancer metastatic to bone has higher expression of the calcium-sensing receptor (CaSR) than primary prostate cancer," *Receptors & Clinical Investigation*, vol. 1, no. 6, p. e270, 2014.
[51] B. Chakravarti, S. K. D. Dwivedi, A. Mithal, and N. Chattopadhyay, "Calcium-sensing receptor in cancer: good cop or bad cop?" *Endocrine*, vol. 35, no. 3, pp. 271–284, 2009.
[52] S. Das, P. Clézardin, S. Kamel, M. Brazier, and R. Mentaverri, "The CaSR in pathogenesis of breast cancer: a new target for early stage bone metastases," *Frontiers in Oncology*, vol. 10, p. 69, 2020.
[53] J. Feng, X. Xu, B. Li et al., "Prostate cancer metastatic to bone has higher expression of the calcium-sensing receptor (CaSR) than primary prostate cancer," *Receptors & Clinical Investigation*, vol. 1, no. 6, p. e270, 2014.
[54] B. S. Mulholland, M. R. Forwood, and N. A. Morrison, "Monocyte chemoattractant protein-1 (MCP-1/CCL2) drives activation of bone remodelling and skeletal metastasis," *Current Osteoporosis Reports*, vol. 17, no. 6, pp. 538–547, 2019.
[55] J. J. Yin, K. Selander, J. M. Chirgwin et al., "TGF-β signaling blockade inhibits PTHrP secretion by breast cancer cells and bone metastases development," *Journal of Clinical Investigation*, vol. 103, no. 2, pp. 197–206, 1999.
[56] A. Schmid-Alliana, H. Schmid-Antomarchi, R. Al-Sahlanee, P. Lagadec, J. C. Scimeca, and E. Verron, "Understanding the progression of bone metastases to identify novel therapeutic targets," *International Journal of Molecular Sciences*, vol. 19, no. 1, p. 148, 2018.
[57] C. Yi, Y. Wang, C. Zhang et al., "Cleavage and polyadenylation specific factor 4 targets NF-κB/cyclooxygenase-2 signaling to promote lung cancer growth and progression," *Cancer Letters*, vol. 381, no. 1, pp. 1–13, 2016.
[58] J. Kular, J. Tickner, S. M. Chim, and J. Xu, "An overview of the regulation of bone remodelling at the cellular level," *Clinical Biochemistry*, vol. 45, no. 12, pp. 863–873, 2012.
[59] Yu-ping Zhu, T. Shen, Ya-jun Lin et al., "Astragalus polysaccharides suppress ICAM-1 and VCAM-1 expression in TNF-α-treated human vascular endothelial cells by blocking NF-κB activation," *Acta Pharmacologica Sinica*, vol. 34, no. 8, pp. 1036–1042, 2013.
[60] H. Qiu, L. Zhang, X. He et al., "Promotion of angiogenesis in vitro by Astragalus polysaccharide via activation of TLR4 signaling pathway," *Journal of Food Biochemistry*, vol. 46, no. 10, Article ID e14329, 2022.
[61] https://www.researchsquare.com/article/rs-1159401/v1.